

Space Potential Distribution in the ISX-B Tokamak

G. A. Hallock,^(a) J. Mathew, W. C. Jennings, and R. L. Hickok
Rensselaer Polytechnic Institute, Troy, New York 12181

and

A. J. Wootton^(a) and R. C. Isler
Oak Ridge National Laboratory, Oak Ridge, Tennessee 37830
 (Received 20 May 1985)

Plasma potentials have been measured for the first time in neutral-beam-heated tokamak discharges, with a heavy-ion beam probe. Radial profiles of these potentials are presented for coinjection, counterinjection, and balanced injection, and for plasmas having only Ohmic heating. They are found to be very dependent on the direction of rotation with respect to the plasma current. They are also found qualitatively consistent with those inferred from radial momentum balance with use of the measured toroidal rotation velocity.

PACS numbers: 52.55.Fa, 52.30.Bt, 52.70.Nc

Detailed scaling experiments from several tokamaks show that neutral-beam injection significantly decreases the global energy confinement times from the values obtained in Ohmically heated discharges.¹ Plasma rotation induced by unidirectional injection has been suggested as a possible cause.² In order to explore this conjecture, a beam line with its direction of injection opposing that of two existing beam lines was added to the Impurity Studies Experiment-B (ISX-B) tokamak. This has allowed us to investigate plasmas having corotation, counterrotation, and almost zero rotation relative to the direction of the Ohmic current. One aspect of characterizing plasma parameters during these studies has involved the measurement of spatially resolved potentials. In this paper we present these measurements and compare them with the potentials inferred from momentum balance. Our studies have been performed in plasmas having a total beam power P_b of 0.8–0.9 MW, beam energy $E_b = 36$ keV, plasma current $I_p = 150$ kA, plasma density $n_e \sim 4 \times 10^{13}$ cm⁻³, and toroidal field $B_\phi = 12.3$ kG. In all cases the working gas is deuterium and the beams are hydrogen.

A heavy-ion beam probe (HIBP) is used to determine the plasma potential as a function of minor radius.³ Singly charged primary ions are injected into the plasma, and the energy differences between this probing beam and doubly charged secondary ions, generated by electron-impact ionization, are measured to obtain the space potential. A schematic drawing is shown in Fig. 1. A 25- μ A, 160-keV Cs⁺ beam is employed. The figure also shows the path along which the potential is determined. It is not possible to probe closer to the center of most plasmas than $\rho = r/a \sim 0.4$, because of beam attenuation. Volume resolution is about 0.1 cm³. Radial profiles are obtained in a single shot, with a scan time of approximately 10 ms during the quasisteady phase of a discharge. Ultraviolet radiation from the discharges modifies the characteristics of the analyzer, but we have developed a calibration pro-

cedure for applying appropriate systematic corrections to the data.⁴

The measured potential profiles are shown in Fig. 2. The uncertainty is ± 100 V for Ohmic discharges, where the ultraviolet loading is small, and ± 400 V for neutral-beam cases, where the systematic corrections are large. Spatial uncertainty is ± 2 cm. All profiles are normalized to zero at $\rho = 1$ (the limiter), because only accurate relative measurements are possible with the applied corrections. The plasma potential at $\rho = 0.4$ is negative with respect to the limiter in all

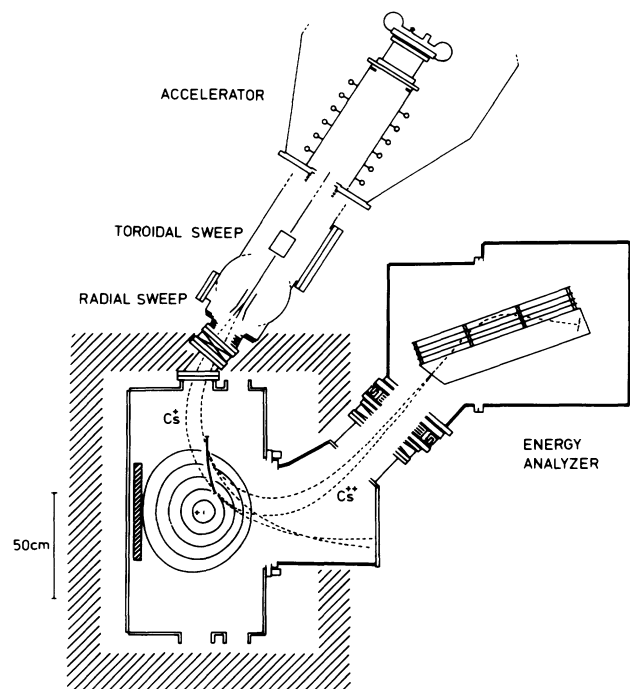


FIG. 1. Schematic diagram of the ISX-B heavy-ion beam probe, and flux-surface plot indicating the measurement scan line.

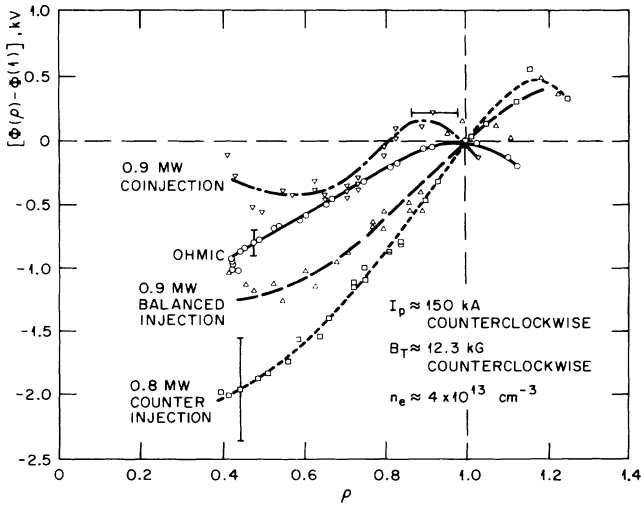


FIG. 2. Measured space potentials with zeros set at the outermost flux surface.

cases, but is much deeper for counterinjection than for coinjection. The values for nonrotating plasmas (balanced injection and Ohmic) are between these limits.

In order to examine whether the measured potentials are consistent with theoretical expectations, we evaluate the ion radial momentum-balance equation for circular plasmas. The flux-surface-averaged equation in steady state is⁵

$$-\frac{\partial \Phi}{\partial r} = \frac{1}{en_i} \frac{\partial P_i}{\partial r} + \langle V_{\phi i} B_{\theta} \rangle - \langle V_{\theta i} B_{\phi} \rangle, \quad (1)$$

where e , n_i , and P_i are the elementary charge, ion density, and scalar ion pressure, respectively, Φ is the electrostatic potential, B_{θ} and B_{ϕ} the poloidal and toroidal magnetic fields, and $V_{\theta i}$ and $V_{\phi i}$ the poloidal and toroidal plasma rotation velocities. We use measured data for the toroidal rotation, and modeling results for the ion pressure and density.

The ion temperature, ion density, and poloidal magnetic field are obtained with the time-independent ZORNOC analysis code.⁶ The ion temperature profile, $T_i(r)$, is obtained from power-balance modeling and the central ion temperature (from charge-exchange measurements). The ion density is obtained from quasineutrality (assuming oxygen is the only impuri-

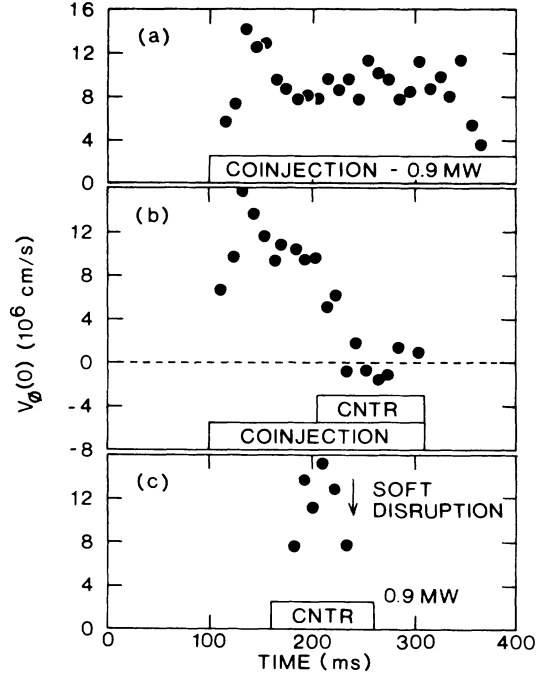


FIG. 3. Magnitudes of central toroidal rotation velocities obtained from Doppler shifts of O VIII CXE lines.

ty), the measured electron density profile (from interferometers), and a neoclassical conductivity model for an assumed constant Z_{eff} . For beam-heated discharges the fast ions are assumed to slow down only through classical collisions. The flux-surface-averaged value of B_{θ} is given by $\langle B_{\theta} \rangle = \mu_0 I(\rho) / l(\rho)$, where $I(\rho)$ is the current enclosed by the flux surface with circumference $l(\rho)$. The current profile consistent with the observed location of the $q = 1$ surface (from soft x-ray diagnostics) and magnetic measurements providing the shape of the outermost flux surface is modeled by the analysis code. Values of these parameters are given in Table I. To reduce modeling inaccuracies due to impurity accumulation and profile variations of Z_{eff} in counter discharges, measurements are obtained as early as possible.

The determination of toroidal rotation has improved significantly from initial efforts.⁷ The central rotation is obtained from Doppler shifts of charge-exchange-

TABLE I. Central values of plasma parameters used in calculating the space potential from the ion momentum balance.

	T_e (eV)	T_i (eV)	n_e (cm^{-3})	n_i (cm^{-3})	I_p (kA)	Z_{eff}
Ohmic	550	396	5.0×10^{13}	4.0×10^{13}	145	2.4
Balanced injection	660	635	5.3×10^{13}	4.8×10^{13}	149	1.1
Coinjection	840	740	5.8×10^{13}	5.1×10^{13}	150	1.2
Counterinjection	580	483	4.8×10^{13}	4.2×10^{13}	143	1.4

excitation (CXE) impurity spectral lines, while Doppler shifts of electron-excited recycling impurities are used elsewhere.⁸ Profiles of $V_\phi(r)$ are relatively broad, and can be approximated by a parabolic function $V_{\phi i} = V_{\phi 0}(1 - \rho^2)^\alpha$, where $0.84 < \alpha < 1.25$ and we take $\alpha = 1$. Because of strong interspecies frictional coupling, we estimate that the difference of V_ϕ between impurities and main ions is less than 3×10^5 cm/s. Figures 3(a) and 3(c) indicate that for coinjection and counterinjection, $V_{\phi 0} \sim 1.2 \times 10^7 \pm 1.5 \times 10^6$ cm/s with fluctuations of 20%. For counterinjection the plasma always disrupts because of impurity accumulation⁷ before steady rotation is reached [Fig. 3(c)]. Potential measurements have concentrated on gettered discharges. The rotation studies in ISX-B were performed in different, mostly nongettered, discharges. However, the measured central rotation is almost independent of controllable plasma parameters (n_e , P_b , I_p , and gettering), and profile variations as a function of these variables appear to be minor. For balanced injection, Fig. 3(b), the rotation is zero within experimental uncertainty. Similarly, any rotation of Ohmically heated discharges is less than 5×10^5 cm/s.

Poloidal rotation above the instrumental limitation of 5×10^5 cm/s (Cv, 2271 Å) has not been detected in ISX-B. For Ohmically heated plasmas the third term in Eq. (1) is estimated from an expression by Hirshman,⁹

$$\langle V_{\theta i} B_\phi \rangle \approx -\frac{1}{e} \left(\frac{\mu_{2i}}{\mu_{1i}} \right) \frac{\partial T_i}{\partial r}, \quad (2)$$

where μ_{1i} and μ_{2i} are the ion parallel viscosity coefficients resulting from particle flow and heat flux. Calculated values of $V_{\theta i} \sim 2 \times 10^5$ cm/s for Ohmic heating cause the potential well to be "deepened" by ~ 200 V. Equation (2) is not valid for beam-heated discharges because of momentum input and anomalous viscosity. For these discharges we take this term equal to zero.

The measured potentials and toroidal rotation show considerable time evolution during a coinjection discharge. Three radial scans, separated in time by 10 ms, are shown in Fig. 4 for the various cases. The plasma current, loop voltage, and line-averaged electron density were essentially constant. The relative change in the potentials is small, except during coinjection. Very limited studies have also indicated that T_i exhibits variations of 200–400 eV in the outer one-third of the plasma during the "quasisteady" period of a coinjected discharge.

Potentials calculated from integrating Eq. (1) and measurements from the heavy-ion beam probe are compared in Fig. 5. For Ohmically heated discharges, where uncertainties are smallest, agreement is excellent. For balanced injection, the measurement and calculations do not match well. The general trend

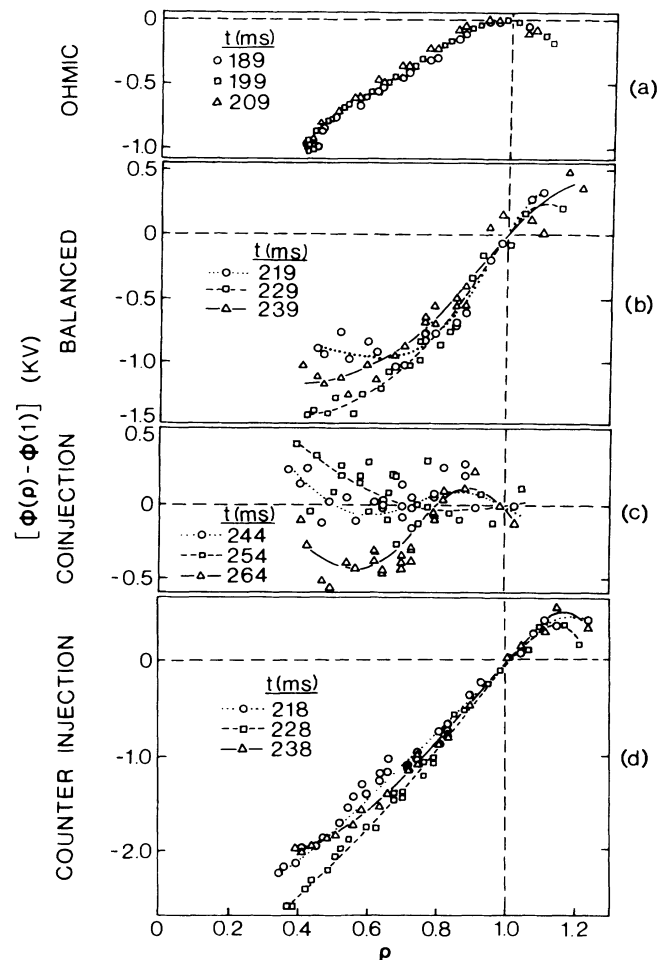


FIG. 4. Measured space-potential evolution during the flat-top portion of the discharges.

agrees, however, with the potential decreasing toward the plasma center. For coinjection the large fluctuations in the measured potential make direct comparisons difficult, since data are not being compared for the same time in the same set of discharges. The profile obtained at 254 ms, however, is consistent with the calculations. In the case of counterinjection, where the first two terms in Eq. (1) have the same sign, the agreement is relatively good [Fig. 5(d)]. For this case it has been necessary to assume that the rotation profile is the same as for coinjection. The profiles cannot be evaluated directly because the location of the radiating ion shifts drastically during a discharge.

The uncertainties of both the HIBP data and of the other plasma parameters are greater in neutral beam discharges than in Ohmically heated discharges. They are difficult to evaluate, particularly for coinjection where $\Phi(r)$ primarily results from the difference of two comparable quantities. We conservatively estimate the uncertainties in the calculated values to be ± 650 V with beam injection and ± 100 V for Ohmic

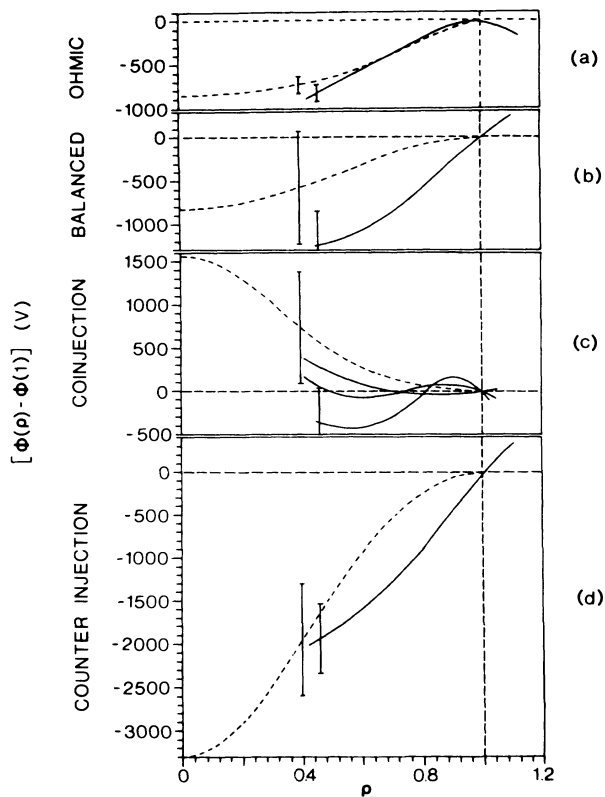


FIG. 5. Comparison of calculated (dashed) and measured (solid) potential profiles. Experimental rotation velocities of (a), (b) 0, (c) $1.2 \times 10^7(1-\rho^2)$ cm/s, and (d) $-1.2 \times 10^7(1-\rho^2)$ cm/s were used to obtain the calculated curves.

discharges.

In summary, the trends expected for corotating, counterrotating, and nonrotating plasmas are confirmed by HIBP results. The large uncertainties of several parameters, however, make it difficult to obtain precise comparisons of the measured plasma po-

tentials with calculations from the radial momentum balance. These results strongly substantiate previous suggestions that impurity behavior in ISX-B^{7,10} is controlled by beam-driven neoclassical effects^{11,12} because the ordering and magnitudes of the potentials that we have directly observed are necessary to the physical processes predicted by these theories.

The authors would like to thank the Fusion Energy Division of the Oak Ridge National Laboratory for their support. Thanks are due P. H. Edmonds, J. C. Forster, K. A. Kannan, J. F. Lewis, E. A. Marguerat, J. K. Munro, M. Murakami, T. F. Rayburn, D. J. Sigmar, R. B. Wysor, and J. L. Yarber for their assistance. This work was sponsored by the U.S. Department of Energy under Contract No. DE-AC05-84OR21400 with Martin Marietta Energy Systems, Inc.

(a) Present address: The University of Texas, Austin, Tex. 78712.

¹G. H. Neilson *et al.*, Nucl. Fusion **23**, 285 (1983).

²M. Murakami *et al.*, in *Proceedings of the Ninth International Conference on Plasma Physics and Controlled Nuclear Fusion Research, Baltimore, 1982* (International Atomic Energy Agency, Vienna, 1983), Vol. 1, p. 57.

³F. C. Jobses and R. L. Hickok, Nucl. Fusion **10**, 195 (1970).

⁴J. Mathew *et al.*, IEEE Trans. Plasma Sci. **13**, 45 (1985).

⁵S. I. Braginskii, Rev. Plasma Phys. **1**, 205 (1965).

⁶R. M. Wieland *et al.*, Nucl. Fusion **23**, 447 (1983).

⁷R. C. Isler *et al.*, Nucl. Fusion **23**, 1017 (1983).

⁸R. C. Isler and L. E. Murray, Appl. Phys. Lett. **42**, 355 (1983).

⁹S. P. Hirshman, Phys. Fluids **21**, 224 (1978).

¹⁰C. E. Bush *et al.*, Nucl. Fusion **23**, 67 (1983).

¹¹W. M. Stacey, Jr., and D. J. Sigmar, Nucl. Fusion **19**, 1665 (1979).

¹²K. H. Burrell *et al.*, Phys. Rev. Lett. **47**, 511 (1981).